

# Supplementary Information

## Pheromone relay networks in the honeybee: messenger workers distribute the queen’s fertility signal throughout the hive

Thomas O. Richardson, Tomas Kay, Laurent Keller, and Nathalie Stroeymeyt

### Dataset summary

The honeybee data analysed here originate from an experiment first described in Richardson *et al.*, 2022 [29]. Whereas that study investigated the three days following the introduction of the eighth cohort, we here expand this period to include the day of the 8<sup>th</sup> cohort, and the three days immediately before and after it [62]. Extending the study period from 3 to 7 days increased the size of the dataset from  $9.7 \times 10^8$  to  $2.1 \times 10^9$  individual trajectory coordinates (Table S1).

Colony	Colony size (est.)	N tagged bees	N trajectory fixes	Total bee hours
1	3656	768	210 417 744	29 225
2	4676	759	286 141 127	39 742
5	4127	738	201 581 258	27 997
6	3673	793	241 078 887	33 483
9	4813	1531	213 721 061	29 683
10	4851	1261	143 537 639	19 936
12	3527	1288	341 151 386	47 382
16	6291	1217	169 081 050	23 483
17	4851	1267	135 617 714	18 836
18	2867	1271	199 942 358	27 770
$\Sigma$	43 332	10 893	2 142 270 224	297 537

Table S1: **Colony-level data summary.** Colony sizes were estimated on the day of the introduction of the 8th cohort by quadrat sampling. The number of tagged bees represents the count of the unique tagged bees in the colony over the seven observation days. The number of trajectory fixes is the total number of tag positions observed across the seven days.

### Queen state detection

To identify periods of queen activity, we used the *moveHMM* package [34] for *R* to model queen movement as a Hidden Markov Model (HMM). To do so we extracted the sequences of frame-to-frame step-lengths and turn angles from the trajectory of each queen. The step length distributions were highly right-skewed, and contained many zero-distance steps, hence a zero-inflated Gamma distribution was used to model the steps in the HMM. As the empirical distributions of turn angles resembled a normal distribution centered on 0, a zero-centered Von Mises circular distribution was used in the HMM.

As the HMM fitting procedure involves stochastic optimisation, repeating the procedure on the same trajectory typically results in a number of HMMs each with different parameters describing the two states. Therefore, to improve the quality of the chosen HMM we use a two-stage process in which we first fitted 100 HMMs to each daily trajectory, and then calculated the average parameter values across the 100 initial models as starting points for the final fit.

Application of the Viterbi algorithm to the 70 daily queen trajectories identified 333,637 bouts of stationary (S) or travelling (T) behaviour, with a mean per-bout state probability of  $0.92 \pm 0.0002$ . Furthermore, the small standard errors associated with the parameters used to fit the distributions of

27 step lengths and turn angles in each HMM (Table S2) indicated that the two states were consistent  
 28 across queens. The average duration of a stationary bout was longer than the average duration of a  
 29 travelling bout, with all 10 queens spending a slightly greater proportion of their time in the stationary  
 30 state (mean time in state, S; 58%, n=10) (Table S2).

State	Step lengths			Turn angles concentration, $\kappa$	Bout probability	Bout duration (s)
	mean, $\mu$	standard deviation, $\sigma$	zero mass			
T	0.067±0.0049	0.00032±0.0002	0.0096±0.0021	0.88±0.06	0.92±0.01	21±5.2
S	0.0075±0.00036	0.000014±0.00002	0.41±0.038	0.4±0.074	0.89±0.011	30±8.2

Table S2: **Summary of the step length and turn-angle distributions fitted by the hidden Markov models to the daily queen trajectories.** All values are grand means and standard errors, calculated using the 10 means for the individual queens. ‘S’; stationary state. ‘T’; travelling state. The step length distributions were modelled using a gamma distribution, and the turn angle distributions were modelled using a zero-centered Von Mises circular distribution. State probabilities were inferred using the Viterbi algorithm.

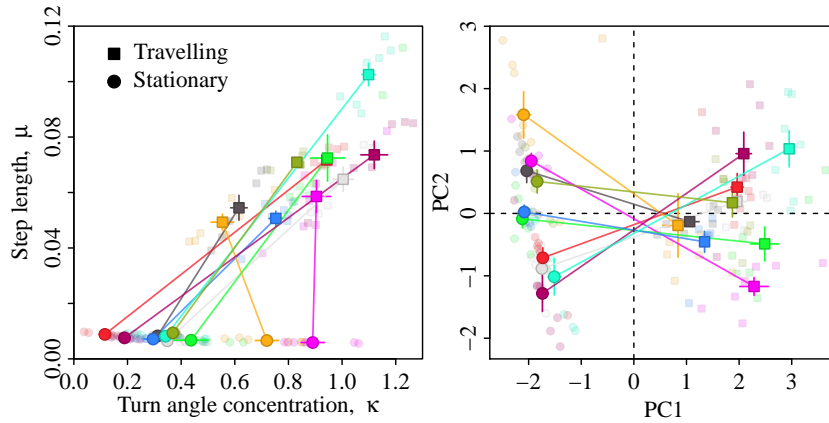


Figure S1: **Summary of two-state Hidden Markov model for queen movement.** (a) The within-bout step length as a function of the within-bout turn angle concentration parameter. Point colours indicate colony identity. Small points indicate the daily means for a single queen, averaged across all bouts. Large points and lines indicate the within-colony grand means and associated standard errors, averaged across the daily means. Lines connect the within-colony grand means. (b) Principal components decomposition of the step length, step length standard deviation, step length zero mass, turn angle concentration, bout probability, and bout duration. The two states are well separated.

## 31 Queen-worker encounter kinetics

32 As the mobility of the honeybee queen has been suggested to play a critical role in the transmission  
33 of the queen pheromone and the rearing of new queens [5,14,18], we investigated how the queen’s  
34 behavioural state influenced her physical encounters with workers. The main paper presented the  
35 statistical analyses showing that honeybee queen encounters are consistently with the predictions of  
36 standard encounter kinetics [35], that is, travelling queens experienced a significantly higher encounter  
37 rate than stationary queens. Figure S2 provides a visual representation of the data on which those  
38 statistical analyses were based.

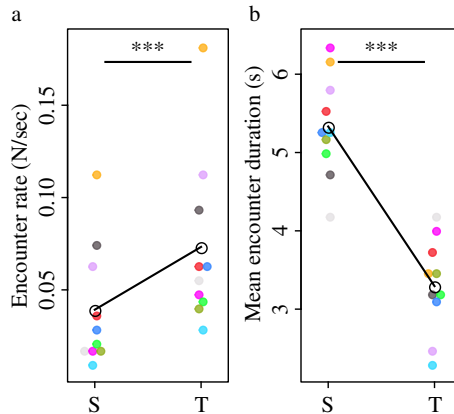


Figure S2: **The behavioural state of the queen influences encounter characteristics.** S: queens in the stationary state. T: queens in the travelling state. Coloured points represent colony means, averaged across the 7 days. Black points indicate grand means, averaged across the 10 colony means. Asterisks indicate the results of the LMMs described in the text (\*\*\*,  $p < 0.0001$ , n.s;  $p > 0.05$ ).

## 39 Community detection and labelling on daily contact networks

40 To identify the optimum number of communities in the daily encounter networks, we measured the soft  
41 modularity [43] associated with FacetNet partitions from 2 to 5 communities. Across all 10 colonies,  
42 the soft modularity exhibited a peak at 3 communities (Fig. S3), so for all analyses we used the  
43 FacetNet partition associated with 3 communities.

44 The FacetNet algorithm provides arbitrary labels to differentiate the communities. Therefore,  
45 following several previous studies [28,29,30,66,67], we used several spatial and demographic features  
46 of the unlabelled communities to assign them to biologically meaningful categories. Social insect  
47 colonies are characterised by a basic distinction between young workers at the core of the nest (nurses)  
48 and older, more peripheral workers (foragers) [26,27], we defined five metrics expected to be tightly  
49 correlated with the nurse-forager axis, namely;

- 50 1. Age (older for foragers)
- 51 2. Number of side switches (more for foragers)
- 52 3. Mean distance to the nest entrance (shorter for foragers)
- 53 4. Mean distance to the nest interior walls (shorter for foragers)
- 54 5. Proportion of time spent inside the broodnest (less for foragers)

55 The rank-order of each community within each metric was then obtained, and the five ranks of each  
56 community summed. Thus, a community whose members were the oldest, switched sides the most,  
57 were closest to the nest entrance and to the nest walls, and that spent least time in the broodnests,  
58 achieved a summed rank of 15. The community with the highest summed rank was then labelled  
59 the ‘Forager’ community. As the members of the remaining two communities typically spent a large  
60 amount of time inside one or both of the two broodnests, we labelled these ‘Nurse A’ and ‘Nurse B’  
61 communities. After labelling, the FacetNet community scores were used as a quantitative indicator of  
62 the affiliations of each individual to the forager (F), Nurse A ( $N_A$ ) and Nurse B ( $N_B$ ) communities.

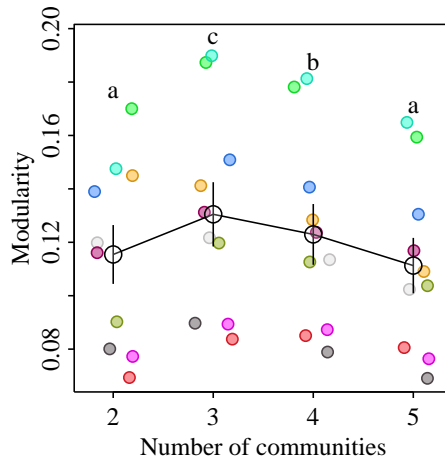


Figure S3: **Honeybee contact networks consist of three partially-overlapping communities.** The y-axis shows the ‘soft’ modularity as a function of the number of communities detected by the Facetnet algorithm. Colours represent colony identities. Each point represents the mean modularity for a given colony, with the mean calculated across the 7 daily networks spanning a three-day period before and after the introduction of the 8th cohort of - day-old tagged callow workers. White points the grand means calculated across the 10 colony means, and the bars give the standard errors thereof. Lower-case letters indicate Tukey post-hoc contrasts applied to a linear mixed model in which the response was modularity and the predictor was the number of communities, and where colony identity was a random effect ( $\chi^2 = 57$ , d.f. = 1,  $p < 0.0001$ ).

63 Although the community affiliations of the queen were not used to help label the communities, in  
 64 all 70 daily networks the queen always exhibited stronger ties to the nurse communities than to the  
 65 forager community.

### 66 A simulation model for queen signal transmission

67 To simulate the transmission of queen pheromones over the time-ordered contact sequences, we devel-  
 68 oped a temporally-explicit stochastic model inspired from standard temporal Susceptible-Infectious  
 69 epidemiological models and parameterised using published experimental data (see below).

70 In our model, the queen was the only primary source of *de novo* pheromone. The amount of  
 71 pheromone carried by the queen was considered to be at equilibrium [16] and had a constant value of  
 72  $\lambda_{queen}$  throughout the simulations. By contrast, workers could acquire pheromone either directly from  
 73 the queen or indirectly from other workers, and pheromone carried by workers experienced a constant  
 74 exponential decay with rate  $k$ . At the onset of each simulation, the queen was initialized with load  
 75  $\lambda_{queen}$  whilst all workers were initialized with a zero load.

76 We then considered all tracking frames sequentially and for each frame  $n$ , we performed the  
 77 following steps in order.

#### 78 (i) Pheromone decay

79 First, the loads of all pheromone-carrying worker bees were updated to account for decay according  
 80 to the following formula:

$$\lambda_{i,n} = \lambda_{i,n-1} \cdot e^{-k(t_n - t_{n-1})},$$

81 where  $\lambda_{i,n}$  is the load of worker  $i$  at tracking frame  $n$  occurring at time  $t_n$ , and  $\lambda_{i,n-1}$  is the load of  
 82 worker  $i$  at the previous frame  $n - 1$  occurring at time  $t_{n-1}$ , and  $k$  is the decay rate. The parts of  
 83 each worker’s load originating directly from the queen or indirectly from workers were also updated  
 84 to account for decay using the same approach.

## 85 (ii) Identifying all pairs of bees in contact and initialising new contact pairs

86 Using the list of sequential contacts extracted from the tracking data, we identified all pairs of bees  
87 that were in physical contact at frame  $n$ , that is, all pairs of bees who had a contact starting at or  
88 before frame  $n$  and ending at or after frame  $n$ .

89 If frame  $n$  was the first frame of a focal contact, we determined which bee of the pair was the  
90 potential donor and which was the potential receiver. As pheromone transfer typically occurs via  
91 the receiver licking or antennating the donor, we used the geometric configuration of the two bees  
92 to identify the potential donor and receiver. More specifically, if only one of the two bees' heads  
93 overlapped with the other's body, then the former was considered as the potential receiver and the  
94 latter as the potential donor. By contrast, if both bees' heads overlapped with the other's body, then  
95 the bee with the higher load was considered as the potential donor.

96 As licking is associated with a pheromone transfer efficiency several orders of magnitude greater  
97 than antennating [16], it was necessary to estimate the proportion of time that the receiver bee spent  
98 licking (rather than antennating) the donor, to obtain a more accurate estimate of the amount of  
99 pheromone transferred during the focal contact. To do so, we used previous empirical data showing a  
100 tight positive association between the duration of the contact and the proportion of time spent licking  
101 [5]. Therefore, if frame  $n$  was the first frame of the focal contact, we also calculated the proportion  
102  $p_{lick}$  of time spent licking as a function of the total duration of the focal contact, using the following  
103 equation (see 'Model parameterisation' section below for details):

$$p_{lick} = \beta + (1 - \beta) \cdot (1 - e^{-\frac{\Delta t}{\tau}})$$

104 where  $p_{lick}$  is the proportion of time spent licking during the focal contact,  $\beta$  is the probability of  
105 licking for instantaneous (zero-duration) contacts,  $\Delta t$  is the duration of the focal contact, and  $\tau$  is the  
106 half-life constant ( $\tau = \frac{(1-\beta)}{2}$ ).

107 Finally, if frame  $n$  was the first frame of the focal contact, the donor load available for transfer,  
108  $\lambda'_{donor}$ , was considered to be equal to the whole donor load,  $\lambda_{donor}$ , at frame  $n$  (see below).

## 109 (iii) Determining the amount of pheromone transferred for each pair of bees in contact

110 We then iterated over all pairs of bees that were in contact at frame  $n$ . For each focal pair of bees,  
111 we first determined whether any pheromone was transferred at frame  $n$ . Transfer occurred if the two  
112 following conditions were met: (i) the potential receiver was not the queen; and (ii) the available load  
113  $\lambda'_{donor}$  of the potential donor at frame  $n$  was higher than the load threshold  $\lambda_{min}$ .

114 If both conditions were met, we next determined whether frame  $n$  corresponded to licking or  
115 antennating for the focal pair of bees. This was determined via a uniform stochastic process with a  
116 probability of licking of  $p_{lick}$ , determined when initialising the focal contact as explained above.

117 We then calculated and recorded the amount of pheromone  $\lambda_{transferred}$  transferred from the donor  
118 to the receiver at frame  $n$  using the following formula:

$$\lambda_{transferred} = \gamma_{type} \cdot \lambda'_{donor}$$

119 where  $\gamma_{type}$  is the per-frame transfer rate for either licking or antennating frame (see below for param-  
120 eterisation), and  $\lambda'_{donor}$  is the donor load available for transfer at frame  $n$ .

## 121 (iv) Updating the loads of donor and receiver bee

122 Once the amount of pheromone transferred from the donor to the receiver was determined, the loads  
123 of both donor and receiver bees were updated as follows:

$$\begin{aligned}\lambda_{donor} &= \lambda_{donor} - \lambda_{transferred} \text{ (except if donor = queen) ;} \\ \lambda'_{donor} &= \lambda'_{donor} - \lambda_{transferred} \text{ (except if donor = queen);} \\ \lambda_{receiver} &= \lambda_{receiver} + \lambda_{transferred} \cdot (1 - p_{ingested})\end{aligned}$$

124 where  $p_{ingested}$  is the proportion of queen pheromone directly ingested by the receiver upon contact,  
125 which is never available for transfer to other individuals (see below). If the donor was the queen, then

126 its total load  $\lambda$  and its load available for transfer  $\lambda'$  remained unchanged and equal to  $\lambda_{queen}$ .

127 Furthermore, depending on whether the donor was the queen or a worker, we calculated the total  
128 amount of pheromone carried by the receiver at frame  $n$  which originated directly from the queen or  
129 indirectly from a worker as follows:

$$\begin{aligned}\lambda_{receiver,queen} &= \lambda_{receiver,queen} + \lambda_{transferred} \cdot (1 - p_{ingested}) \text{ if donor} = \text{queen;} \\ \lambda_{receiver,worker} &= \lambda_{receiver,worker} + \lambda_{transferred} \cdot (1 - p_{ingested}) \text{ if donor} = \text{worker}\end{aligned}$$

130 Finally, if the focal contact at frame  $n$  was labelled as licking, then the donor load available for  
131 transfer was further updated as follows, to reflect the observation that during a prolonged contact the  
132 pheromone is becoming increasingly difficult to acquire by the receiver (see parameterisation below):

$$\lambda'_{donor} = \lambda'_{donor} \cdot \left(1 - \frac{\alpha}{2i}\right)$$

133 where  $\alpha$  is an attenuation rate and  $i$  is the cumulated of licking frames since the beginning of the focal  
134 contact (see parameterisation below).

135 After updating the loads of the donor and receiver, the next pair of bees in contact at frame  $n$  was  
136 considered and we repeated steps (iii-iv) until all pairs of bees in contact at frame  $n$  were treated.

### 137 (v) Ending contacts

138 Using the list of sequential contacts extracted from the tracking data, we identified all pairs of bees  
139 who had a physical contact that ended at frame  $n$ . For all ending contacts, we recorded the total  
140 (cumulated) amount of pheromone transferred during the contact.

### 141 (vi) Recording loads

142 Once all contacts at frame  $n$  were processed, we recorded the load of each bee at the end of frame  $n$ ,  
143 as well as what proportion of its current load originated from a direct transfer from the queen or from  
144 an indirect transfer from a worker.

145 We then considered the next tracking frame  $n+1$  and repeated steps (i-vi) until all tracking frames  
146 were processed.

## 147 Model parameterisation

- 148 •  $\lambda_{queen} = 423$  ng (from Naumann *et al.*, 1991 [16]).
- 149 • The pheromone decay rate  $k$  was calculated as the sum of the decay rates associated with two  
150 complementary processes: (i) internalization of the pheromone through the cuticle (parameter  
151  $k_2 = 6.8 \times 10^{-4} s^{-1}$  in [16]) and (ii) deposition of the pheromone on the wax (parameter  $k_6 =$   
152  $1.31 \times 10^{-4} s^{-1}$  in [16]). This led to a total decay rate  $k = k_2 + k_6 = 8.11 \times 10^{-4} s^{-1}$ , which  
153 corresponds to a half-life on the worker cuticle of about 14.24 min.
- 154 • To evaluate the proportion of time spent licking (rather than antennating) during a focal contact,  
155 we used published empirical on the total length of time that individual bees spent licking or  
156 antennating the queen during any single contact (Table IIIb in Butler, 1954 [5]). As the shortest  
157 contact recorded by Butler lasted 10 seconds, whilst the shortest contacts recorded by our  
158 tracking systems lasted 0.5 second (single frame contacts), we added one additional data point  
159 to this dataset, assuming that a single frame contact is too short to allow licking and thus  
160 involves antennation only. We then used the Nonlinear Least Squares estimation (function `nls`  
161 from package `stats` in R version 4.2.1) to fit an equation of the form  $p_{lick} = \beta + (1 - \beta) \cdot (1 - e^{-\frac{\Delta t}{\tau}})$   
162 to the dataset, where  $p_{lick}$  is the proportion of time spent licking during a single focal contact,  $\beta$   
163 is the probability of licking for instantaneous (zero-duration) contacts,  $\Delta t$  is the duration of the  
164 focal contact, and  $\tau$  is the half-life constant ( $\tau = \frac{(1-\beta)}{2}$ ). The best fit had parameter values  $\beta$   
165  $= 0.249$  and  $\tau = 88.76$  seconds (Fig. S4). Using these parameter values and the equation above,  
166 it was possible to infer  $p_{lick}$  for any focal contact in our dataset based on its duration  $\Delta t$ .

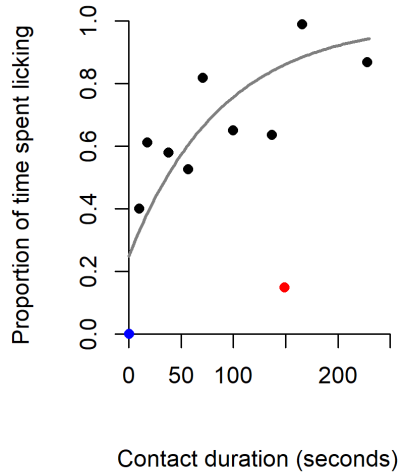


Figure S4: **Model parameterisation: relationship between contact duration and time spent licking.** Black points: data from Butler (1954) used in parameterisation; red point: outlier in data from Butler (1954), not used in the parameterisation; blue point: extra data point for single-frame contact; grey line: line of best fit with parameter values  $\beta = 0.249$  and  $\tau = 88.76$  seconds.

- 167 •  $\lambda_{min}$ , the minimum donor load for which a transfer occurred, was defined as the bees' sensitivity  
 168 threshold for the queen pheromone as determined by Kaminski *et al.*, (1990) [38], i.e.:

$$\lambda_{min} = 10^{-7} \cdot 1 \text{ Qeq}$$

169 where 1 *Qeq* is one 'queen equivalent', that is, the average content of the mandibular gland of  
 170 one mated honeybee queen. Following [16], we used a value of 1*Qeq* = 90.3*μg*.

- 171 •  $p_{ingested} = 0.5$  according to [16]
- 172 • To parameterise the per-frame transmission rate for licking and antennating contacts, we used  
 173 empirical data provided by [16] for the pheromone load carried by receiver bees after prolonged  
 174 contacts of 5s, 30s and 60 s with a dead worker bee to which 250ng of traceable (tritiated) queen  
 175 pheromone had been applied (Figure 4 in [16]), and after 5-second antennation-only contacts  
 176 with a lure to which 8.5ng of traceable (tritiated) queen pheromone had been applied. To be  
 177 consistent with our tracking data and simulations, all contact durations were first converted  
 178 from seconds to frames using our tracking frame rate of 2 frames per second (hence a five-second  
 179 contact was considered to last 10 frames). In a first parameterisation attempt, we considered a  
 180 constant per-frame rate of transfer for antennation and licking. Using the 5-second antennation-  
 181 only empirical contact data led to an estimated per-frame rate of transfer for antennation of  
 182  $1.765 \text{ frame}^{-1}$ . We then calculated the expected proportion of time spent licking vs. anten-  
 183 nating for each contact duration in the prolonged contact empirical dataset (5s, 30s, 60s) using  
 184 the equation and parameter values described above. Using the expected proportion of time  
 185 spent licking in 5-second prolonged contacts and a per-frame rate of transfer for antennation  
 186 of  $\gamma_{antennation} = 1.765 \times 10^{-5} \text{ frame}^{-1}$ , we estimated a per-frame rate of transfer for licking  
 187  $\gamma_{licking} = 0.0125 \text{ frame}^{-1}$ . However, these estimates led to an increasingly large over-estimation of  
 188 the receiver loads for longer contacts, suggesting that the queen pheromone becomes increasingly  
 189 hard to acquire by the receiver during prolonged contact, e.g. because licking quickly exhausts  
 190 the amount of easily accessible pheromone at the point of contact between the two bees. We  
 191 therefore assumed that the amount of pheromone available for transfer on the source declined

192 at an increasing rate over time during a single prolonged contact, according to the following  
193 formula:

$$\lambda'_{\text{source}} = \lambda'_{\text{source}} \cdot \left(1 - \frac{\alpha}{2i}\right)$$

194 where  $\lambda'_{\text{source}}$  is the load of the source at the end of a licking frame, and  $i$  is the total, cumulated  
195 number of licking frames since the beginning of the contact. A starting value for parameter  
196  $\alpha$  was computed using non-linear least squares estimation of the difference between our pre-  
197 dicted load and the receiver load measured in the empirical dataset, after taking into account  
198 the constant pheromone decay with parameter  $k$ . We then used a step-by-step approach simu-  
199 lating the receiver load for various combinations of parameters values for  $\gamma_{\text{antennation}}$ ,  $\gamma_{\text{lick}}$  and  
200  $\alpha$ , and selected the final parameter values that produced the lowest sum-of-square differences  
201 between predicted and empirical values. The final chosen parameter values were the following:  
202  $\gamma_{\text{antennation}} = 7.059 \times 10^{-5} \text{ frame}^{-1}$ ,  $\gamma_{\text{lick}} = 0.021$ , and  $\alpha=1.057$ . Figure S5 shows the final fit  
203 between the predicted and empirical values.

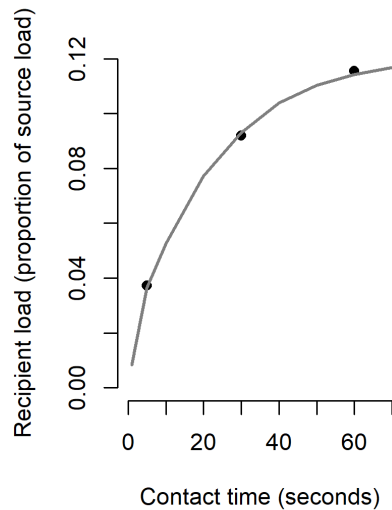


Figure S5: **Model parameterisation: diminishing transmission with longer contacts.** Black points: empirical data from Nauman (1991) [16], showing the mean receiver load after three prolonged contact durations, expressed as a proportion of the initial donor load of 250ng. Grey line: simulation outcome with parameter values  $\gamma_{\text{antennation}} = 7.059 \times 10^{-5} \text{ frame}^{-1}$ ,  $\gamma_{\text{lick}} = 0.021 \text{ frame}^{-1}$ , and  $\alpha=1.057$ .



204 **Queen bout durations**

205 Figure S6 shows the queen bout duration distribution, pooled across all colonies, and across both  
 206 stationary and travelling bouts. The distribution is right-skewed, and possesses a long tail.

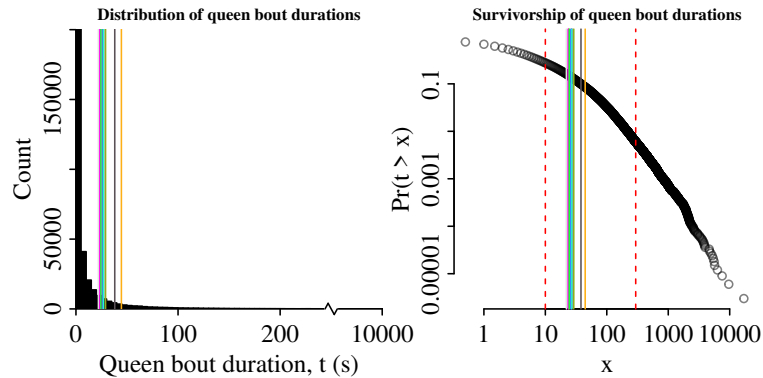


Figure S6: **Distribution of queen bouts.** (a) Frequency distribution of the durations of all queen bouts pooled across all colonies. Solid vertical lines indicate colony medians. (b) Complementary cumulative distribution (i.e., survivorship) for the pooled queen bout duration. Note, both axes have been log-transformed. Dashed red lines indicate the upper and lower cutoffs, at 10 and 305 seconds respectively.

207 **Calculating difference vectors**

208 The difference maps were calculated in two stages. The first was to obtain an overall vector field  
 209 describing the orientations of receivers relative to the messenger. To do so, for each colony on each  
 210 day, we identified all times when a worker occupied a given grid site within the messenger-centric  
 211 coordinate system  $(x, y)$ . We then extracted the receiver headings associated with these visits, to  
 212 obtain a circular distribution,  $P(\theta) \in (-\pi, \pi)$  for each  $(x, y)$  grid, and for each of the 10 colonies.  
 213 This distribution was summarised by a polar vector  $\vec{v} = r\bar{\theta}$ , where the magnitude  $r$  was given by the  
 214 mean resultant length, and the heading  $\bar{\theta}$  was given by the circular mean. We then combined the ten  
 215 within-colony vectors, thus producing a ‘grand mean’ vector (Fig. S7a-b). By sequentially averaging  
 216 in this manner, we ensured equal weighting of all colonies within the overall grand mean.

217 The second stage was to calculate the difference in receiver orientation between pre- versus post-  
 218 encounter messengers, or between post-encounter messengers with a given pheromone load and all  
 219 post-encounter messengers irrespective of load. Thus, for the analysis of the effect of the queen  
 220 encounter upon the messenger’s subsequent encounters, we subtracted the receiver vector for pre-  
 221 encounter messengers from the vector for post-encounter messengers, that is,  $\Delta\vec{v}_{time} = \vec{v}_{post} - \vec{v}_{pre}$ .  
 222 The vector connecting the origin to the end of the reversed pre-encounter vector gives the ‘difference  
 223 vector’,  $\Delta\vec{v}_{time}$  (Fig. S7c).

224 In both of the analyses presented in Figure 4 in the main paper, the difference vector maps  
 225 were conditioned on an additional variable; in the analysis of how a queen encounter influences the  
 226 subsequent encounters of the messenger (Figure 4 a-c), this variable was a sequence of time-windows  
 227 of width  $w = 60$  seconds, covering the 300 second period immediately before and immediately after the  
 228 queen encounter. Difference maps were calculated for each window, by subtracting the pre-encounter  
 229 vectors for the  $n^{th}$  window before the queen encounter from  $n^{th}$  window after it. Thus, the difference  
 230 vector map for the fifth one-minute time window could be written,  $\Delta\vec{v}_{241:300} = \vec{v}_{241:300} - \vec{v}_{-241:-300}$ .

231 In the analysis of how the amount of queen pheromone a messenger carries (its load) influences  
 232 encounters with other workers (Figure 4 d-f), the conditioning variable was given by the deciles of  
 233 the colony load distribution. This was because differences in the number of tagged workers between  
 234 colonies and across days influence the (simulated) volume of the queen pheromone that is in circula-  
 235 tion at a given mement. To facilitate comparisons between days or between colonies, a daily load  
 236 distribution was produced for each colony, and the load carried by a given messenger at a given  
 237 time expressed in terms of the load deciles of this distribution. For the load distribution, we used  
 238 the instantaneous loads (i.e., the frame-by-frame values) of the pre- and post-encounter messengers,

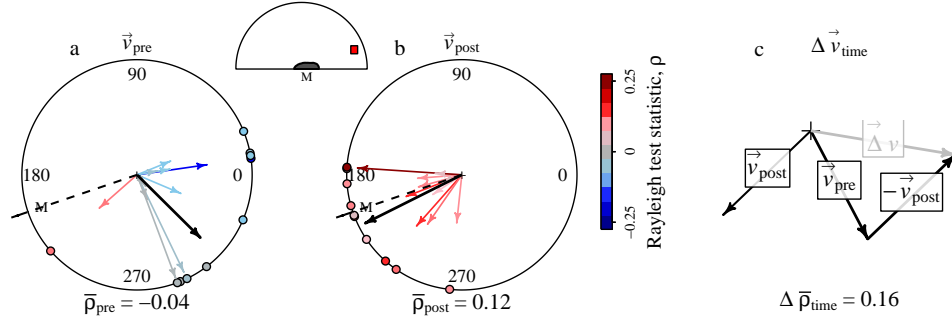


Figure S7: **Calculating difference vectors for receivers orienting towards pre- versus post-encounter messengers.** The two circular plots show the typical orientations of receivers visiting an anterior grid within the messenger-centric coordinate system, as shown by the red square in the upper panel insert. Typical receiver orientations at this site are shown for pre- and post-encounter messengers (panels **a** & **b** respectively). Each coloured arrow represents a polar vector  $\vec{v} = r\bar{\theta}$  for a single colony, where the direction  $\bar{\theta}$  indicates the circular mean of the receiver headings, and the magnitude  $r$  indicates the mean resultant length. Arrow colours indicate the Rayleigh test statistic,  $\rho$ , which measures the extent to which a given vector is oriented towards or away from a specified direction, as provided by the direction from the grid to the messenger (dashed black line, ‘M’). The  $\bar{\rho}$  values below each plot indicate the mean Rayleigh test statistic for the pre- and post-encounter messengers, where each colony contributes one value to the average. The black arrows indicate the ‘grand mean’ vector, obtained by vector addition of the 10 colony vectors. (c) Using vector subtraction to obtain the post-pre ‘difference vector’,  $\Delta\vec{v}$ .

239 obtained from the daily transmission simulations. Thus, the difference vector map for a messenger  
 240 whose current load was greater than 90% of the rest of the workers in their colonies could be written;  
 241  $\Delta\vec{v}_{91:100\%} = \vec{v}_{91:100\%} - \vec{v}_{1:100\%}$ .